Static Subsonic Aeroelastic Stability of a Shell Wrapped Around a Rigid Surface

Earl H. Dowell* and Andrew L. Katz†
Duke University, Durham, North Carolina
and
Robert L. Goldman‡
Martin Marietta Laboratories, Baltimore, Maryland

A thin elastic shell under tension is wrapped around a rigid curved surface; the latter renders the stiffness of the shell effectively nonlinear. Examples of such a configuration in practice include the NASA Skylab Space Project and certain submarine geometries. The static aeroelastic stability of the shell is examined for a subsonic flow along the axis of the shell and the longitudinal axis of the curved rigid surface. The minimum flow velocity for which the elastic shell will deform statically (buckle) is determined, as well as the amplitude of the deformation as a function of flow velocity.

Introduction

In various applications, a thin elastic sheet (an elastic plate under tension) is wrapped around a rigid, curved surface (i.e., a curved surface whose stiffness is much larger than that of the elastic sheet) to form an elastic shell. This rigid surface or mandrel has an important effect on the effective stiffness of the elastic shell and, indeed, renders the stiffness of the shell effectively nonlinear. Examples of such applications include the thermal shield for the NASA Skylab Space Project and also certain acoustical shields in hydronautical environments.

Here the static stability of the shell is examined with a subsonic compressible fluid flowing over and along the axis of the elastic sheet and mandrel. See Fig. 1 for a schematic of the geometry. The elastic shell is curved in the spanwise direction and under tension in both the spanwise directions. The elastic shell is mounted flush with the mandrel surface and, for no fluid flow, remains so in the absence of any manufacturing imperfections in the elastic shell or mandrel. The dashed line indicates a deformation of the shell away from the mandrel.

The present work was motivated by a concern that a thin elastic shell under tension wrapped around a submarine hull might become hydroelastically unstable. The proposed shell geometry for that application is transversely orthotropic (several layers of varying thicknesses, h_1, h_2, and moduli of elasticity, E_1, E_2), but an equivalent isotropic shell is studied in this paper. See Fig. 1.

The flow is taken as uniform and aligned along the axis of the mandrel. Any turbulent fluctuations in the fluid are ignored and, below a certain critical flow speed, the elastic sheet remains undisturbed. Above the critical flow speed, a static aeroelastic instability occurs, and the elastic shell deforms away from the mandrel. It is desired to determine this critical flow speed and the associated deformation pattern of the elastic shell.

If the turbulent fluctuations in the fluid were taken into account, the random forced response of the elastic shell could also be determined. That is a subject for a separate study. Here, only the *static* aeroelastic instability i.e., divergence, is considered. It would be of interest to study the dynamic hydroelastic instability, or flutter, as well. However, on physical grounds and based on earlier research,[1] divergence is expected to be more critical than flutter for this structural geometry and subsonic compressible flow conditions.

Received Aug. 15, 1988; revision received June 12, 1989.

*Dean, School of Engineering. Fellow AIAA.
†Research Assistant.
‡Consultant. Associate Fellow AIAA.

Analysis

After Dowell and Ventres,[2] the equations of equilibrium and compatibility for a curved elastic shell are

$$D\nabla^4 w = \Phi_{yy} w_{xx} - 2\Phi_{xy} w_{xy} + \Phi_{xx} w_{yy} + \bar{p} - \Delta p \tag{1}$$

and

$$\frac{\nabla^4 \Phi}{Eh} = w_{xy}^2 - w_{xx} w_{yy} \tag{2}$$

where subscripts x and y on w, Φ denote derivatives with respect to those spatial variables.

These are basically the von Kármán large deflection plate equations. The various symbols are w, the plate or shell deflection normal to its surface; Φ, the Airy stress function whose existence insures that the in-plane equilibrium equations are satisfied; D, E, h, the plate stiffness, modulus of elasticity and thickness, respectively; $\bar{p}$, a static pressure externally imposed (e.g., by the mandrel) and positive in the same direction as w; and Δp, an aerodynamic pressure due to the flowing fluid and positive in the direction opposite to w.

Note that the in-plane stress resultants, N_x, N_y, N_{xy}, are given in terms of the Airy stress function by

$$N_x \equiv \Phi_{yy}, \qquad N_y \equiv \Phi_{xx}, \qquad N_{xy} \equiv -\Phi_{xy} \tag{3}$$

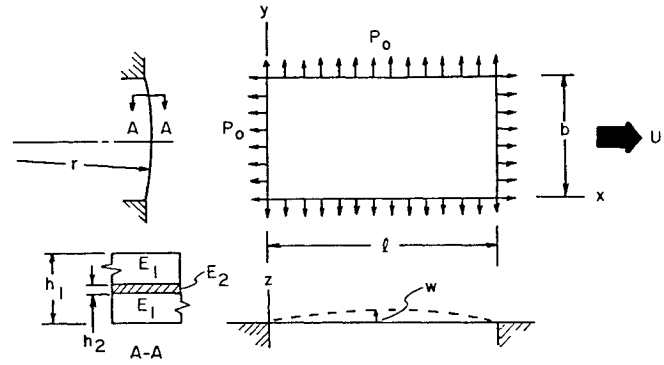

Fig. 1 Model geometry and notation.

These in-plane stress resultants also can be related to the in-plane and bending displacements, i.e.,

$$(1-\nu^2)\frac{N_x}{Eh} = u_x + \frac{1}{2}(w_x)^2 + \nu\left[v_y + \frac{1}{2}(w_y)^2\right]$$

$$(1-\nu^2)\frac{N_y}{Eh} = v_y + \frac{1}{2}(w_y)^2 + \nu\left[u_x + \frac{1}{2}(w_x)^2\right]$$

$$(1-\nu^2)\frac{N_{xy}}{Eh} = 2(1-\nu)[w_x w_y + u_y + v_x] \tag{4}$$

where ν is Poisson's ratio and u, v are the in-plane displacements.

Physical Scenario

It will be helpful conceptually to think of a sequence of steps leading to the physical configuration of interest.

Step I

1) There is no fluid flow; $\Delta p = 0$.
2) There is no mandrel; $\bar{p} = 0$.
3) There is initial tension; $N_{x_I} = \bar{N}_x$, $N_{y_I} = N_y$, and $\bar{N}_{xy_I} = 0$.
4) There is no bending displacement; $w_I = 0$.
5) Equations (1) and (2) are then satisfied trivially.

Step II

1) There is still no fluid flow; $\Delta p = 0$.
2) There is now a mandrel that applies a pressure; $\bar{p} \neq 0$.
3) The corresponding w_{II} and Φ_{II} satisfy, from Eqs. (1) and (2),

$$D\nabla^4 w_{II} = \Phi_{II_{yy}} w_{II_{xx}} - 2\Phi_{II_{xy}} w_{II_{xy}} + \Phi_{II_{xx}} w_{II_{yy}} + \bar{p} \tag{1}_{II}$$

$$\frac{\nabla^4 \Phi_{II}}{Eh} = w_{II_{xy}}^2 - w_{II_{xx}} w_{II_{yy}} \tag{2}_{II}$$

For example, consider a parabolic mandrel shape, i.e.,

$$w_{II} = 4W_{II}\frac{y}{b}\left(1 - \frac{y}{b}\right) \tag{5}$$

where W_{II} is the maximum height and b the span of the curved mandrel and the elastic shell that is wrapped around it. From Eq. (5),

$$w_{II_{yy}} = -8\frac{W_{II}}{b^2} \equiv -\frac{1}{r} \tag{6}$$

where r is the radius of curvature, Equations $(1)_{II}$ and $(2)_{II}$ then become

$$0 = 0 - 0 + N_{y_{II}}\left(-\frac{1}{r}\right) + \bar{p} \tag{1}_{II}$$

and

$$0 = 0 \tag{2}_{II}$$

Thus,

$$N_{y_{II}}\frac{1}{r} = \bar{p} \tag{7}$$

Note that $N_{y_{II}}$ includes the in-plane tension induced by bending as well as the initial in-plane tension $\bar{N}_y$. In practice, the latter may dominate.

At the end of step II, the elastic plate is now curved as a shell and under tension with a pressure load from the mandrel.

Step III

1) The fluid now flows, and an aerodynamic pressure is applied, $\Delta p \neq 0$

2) Let

$$w = w_{II} + w_{III} \tag{8}$$

$$\Phi = \Phi_{II} + \Phi_{III} \tag{9}$$

3) If $w_{III} > 0$, then the curved plate or shell is off the mandrel and $\bar{p} = 0$. Note that if $\Delta p = 0$ (no fluid flow), then the shell will simply return to the mandrel, i.e., $w_{III} = 0$ and $\bar{p} \neq 0$. However, for $\Delta p \neq 0$, an equilibrium position may exist with the shell off the mandrel, $w_{III} > 0$ and $\bar{p} = 0$. Determining this nontrivial equilibrium is a principal goal of this analysis.

Substitute Eqs. (8) and (9) into Eqs. (1) and (2); then, noting $\bar{p} = 0$, one has

$$D\nabla^4(w_{II} + w_{III}) = (\Phi_{II_{yy}} + \Phi_{III_{yy}})w_{III_{xx}} - 2(\Phi_{II_{xy}} + \Phi_{III_{xy}})w_{III_{xy}} + (\Phi_{II_{xx}} + \Phi_{III_{xx}})\left(-\frac{1}{r} + w_{III_{yy}}\right) - \Delta p \tag{10}$$

$$\frac{\nabla^4 \Phi_{III}}{Eh} = (w_{III_{xy}})^2 - w_{III_{xx}}\left(-\frac{1}{r} + w_{III_{yy}}\right) \tag{11}$$

Further, using Eqs. $(1)_{II}$ and $(2)_{II}$ in Eqs. (10) and (11), Eq. (10) becomes

$$D\nabla^4 w_{III} = (\Phi_{II_{yy}} + \Phi_{III_{yy}})w_{III_{xx}} - 2(\Phi_{II_{xy}} + \Phi_{III_{xy}})w_{III_{xy}} + \Phi_{II_{xx}} w_{III_{yy}} + \Phi_{III_{xx}}\left(-\frac{1}{r} + w_{III_{yy}}\right) - \bar{p} - \Delta p \tag{10}$$

and Eq. (11) remains the same.

Before proceeding further with this *nonlinear* analysis, consider briefly the simplifications and approximations associated with a *linear* analysis. A standard linear analysis would be performed by neglecting products of w_{III} and Φ_{III} and their derivatives in Eqs. (10) and (11), i.e.,

$$D\nabla^4 w_{III} = \Phi_{III_{yy}} w_{III_{xx}} - 2\Phi_{xy_{II}} w_{III_{xy}} + \Phi_{II_{xx}} w_{III_{yy}} + \Phi_{III_{xx}}\left(-\frac{1}{r}\right) - \bar{p} - \Delta p \tag{10}_L$$

and

$$\frac{\nabla^4 \Phi_{III}}{Eh} = -w_{III_{xx}}\left(-\frac{1}{r}\right) \tag{11}_L$$

If, in addition, the initial tension dominates with respect to step II, then

$$\Phi_{II_{xx}} = \bar{N}_y, \qquad \Phi_{II_{yy}} = \bar{N}_x, \qquad \Phi_{II_{xy}} = 0 \tag{12}$$

and Eqs. (10_L) and (11_L) can be further simplified. Finally, it is noted that, in a linear stability analysis, an inhomogeneous term (external forcing) such as $\bar{p}$ will have no effect and can be neglected. Thus, in a linear stability analysis, once the mandrel has deformed the plate, it is as though the mandrel's presence has no further effect. More will be said about the comparison of nonlinear and linear theory when the numerical examples are discussed.

Step II Revisited

Now, consider further the in-plane boundary conditions and the determination of $N_{y_{II}}$ and $\bar{p}$. If the in-plane edges of the curved elastic plate are unrestrained, then one may show that

$$N_{y_{II}} = \bar{N}_y \tag{13}$$

and

$$\bar{p} = \bar{N}_y / r$$

where $\bar{N}_y$ is the initial applied in-plane tension.

That the in-plane edges are unrestrained is a reasonable assumption since even thin elastic plates that are flexible in bending are quite stiff with respect to in-plane deformations relative to their supports.

Using Eqs. (12) and (13), Eq. (10) becomes

$$D\nabla^4 w_{\text{III}} = (\bar{N}_x + \Phi_{\text{III}_{yy}})w_{\text{III}_{xx}} - 2\Phi_{\text{III}_{xy}} w_{\text{III}_{xy}} + \bar{N}_y w_{\text{III}_{yy}} + \Phi_{\text{III}_{xx}}\left(-\frac{1}{r} + w_{\text{III}_{yy}}\right) - \frac{\bar{N}_y}{r} - \Delta p$$

(10 free in-plane edges)

Equation (11) remains unchanged, of course.

For additional discussion of in-plane edge boundary conditions and step II, see Appendix A.

Solution Procedure

A Galerkin solution procedure will be followed. It is assumed that the curved plate will deform primarily in its fundamental modal pattern.[2,3] Thus, it is assumed that

$$w_{\text{II}} = w_0 \sin\frac{\pi x}{\ell}\sin\frac{\pi y}{b} \tag{14}$$

and

$$\Phi_{\text{III}} = \Phi_0 \sin\frac{\pi x}{\ell}\sin\frac{\pi y}{b} \tag{15}$$

Note that, for free in-plane edges, only a particular form of the solution for Φ is needed; the homogeneous solution can be taken as trivially zero.

Substituting Eqs. (14) and (15) into Eqs. (10) and (11), multiplying each of the latter by $\sin[(\pi x)/\ell]\sin[(\pi y)/b]$, and integrating over the solution domain (elastic shell area) gives two (nonlinear) algebraic equations for w_0 and Φ_0. In nondimensional form, these are

$$\pi^4 W_0\left[1 + \left(\frac{\ell}{b}\right)^2\right]^2\left(\frac{1}{4}\right) = -R_x\pi^2 W_0\left(\frac{1}{4}\right) + \pi^4\left(\frac{\ell}{b}\right)^2\phi_0\left(\frac{16}{9\pi^2}\right)W_0 - 2\phi_0 W_0\pi^4\left(\frac{\ell}{b}\right)^2\left(\frac{4}{9\pi^2}\right) - R_y\left(\frac{\ell}{b}\right)^2\pi^2 W_0\left(\frac{1}{4}\right) + \pi^2\phi_0\left[\gamma\left(\frac{1}{4}\right) + \pi^2\left(\frac{\ell}{b}\right)^2\left(\frac{16}{9\pi^2}\right)W_0\right] - R_y\gamma\left(\frac{4}{\pi^2}\right) - \int_0^1\int_0^1 \Delta P \sin\frac{\pi x}{\ell}\sin\frac{\pi y}{b}\frac{\mathrm{d}x}{\ell}\frac{\mathrm{d}y}{b} \tag{16}$$

$$\phi_0 = -\left[W_0^2\left(\frac{\ell}{b}\right)^2\left(\frac{4}{\pi^2}\right)\left(\frac{4}{3}\right) + \left(\frac{W_0}{\pi^2}\right)\gamma\right]\Big/\left[1 + \left(\frac{\ell}{b}\right)^2\right]^2 \tag{17}$$

where

$$W_0^2 \equiv w_0^2\frac{Eh}{D}$$

$$\phi_0 \equiv \frac{\Phi_0}{D}$$

$$R_x \equiv \frac{\bar{N}_x\ell^2}{D}$$

$$R_y \equiv \frac{\bar{N}_y\ell^2}{D}$$

$$\gamma \equiv \left(\frac{Eh}{D}\right)^{1/2}\frac{\ell^2}{r}$$

$$\Delta P \equiv \left(\frac{Eh}{D}\right)^{1/2}\frac{\ell^4}{D}\Delta p \tag{18}$$

In the next section, where the aerodynamic modeling is discussed, it will be shown that

$$\int_0^1\int_0^1 \Delta P \sin\frac{\pi x}{\ell}\sin\frac{\pi y}{b}\frac{\mathrm{d}x}{\ell}\frac{\mathrm{d}y}{b} = W_0\lambda\frac{1}{2}(-Cp) \tag{19}$$

where $\lambda \equiv \rho U^2\ell^3/D$, ρ is the fluid density, U is the mean fluid velocity, and $Cp = Cp(\ell/b)$. Cp is defined by Eq. (19).

Thus, from Eqs. (16–19), the functional form of the solution can be written as

$$W_0 = W_0(\lambda, \gamma, \ell/b, R_x, R_y) \tag{20}$$

Indeed, it is seen that, using Eqs. (17) and (19) in Eq. (16), one can obtain a cubic polynomial in W_0, whose roots will give the explicit form of Eq. (20).

Aerodynamic Modeling

The aerodynamic model will be taken from linear, small-perturbation potential flow theory. It can be shown that the aerodynamic nonlinearities are negligible compared to the structural nonlinearities included in the present study.

The *incompressible* potential flow theory is compactly presented as follows:

$$\nabla^2\phi = 0 \tag{21}$$

$$\phi_z|_{z=0} = Uw_x \tag{22}$$

$$\Delta p = -\rho U\phi_x \tag{23}$$

where ϕ is the fluid velocity potential (not to be confused with the Airy stress function). Solving Eq. (21) for ϕ subject to the boundary condition (22), and appropriate finiteness conditions such as $z \to \infty$, determines ϕ in terms of w. Formula (23) may then be used to determine the aerodynamic pressure loading Δp. The general form of the solution is[4]

$$\frac{\Delta p}{\rho U^2} = \int_0^1\int_0^1 A(x-\xi, y-n)w_x(\xi,n)\frac{\mathrm{d}\xi}{\ell}\frac{\mathrm{d}\eta}{b} \tag{24}$$

See Ref. 4 for the explicit form of A. Normally, the integral in Eq. (24) must be evaluated numerically.

Further simplifications are possible. For example, in Eq. (21),

$$\nabla^2\phi \equiv \phi_{xx} + \phi_{yy} + \phi_{zz} = 0 \tag{21}$$

can be approximated by

$$\phi_{xx} + \phi_{zz} = 0 \tag{21_S}$$

This is usually called "strip theory" and is valid for ℓ/b sufficiently small.

Alternatively, Eq. (21) may be approximated by

$$\phi_{yy} + \phi_{zz} = 0 \tag{21_{SB}}$$

This is usually called "slender-body" theory and is valid for ℓ/b sufficiently large.

For simplicity and purposes of illustration, the strip theory approximation will be used here. Then Eq. (24) can be simplified and written in the more explicit form[1,3]

$$\Delta p = -\frac{\rho U^2}{\pi}\int_0^\ell [w_\xi(\xi)/(x-\xi)]\,\mathrm{d}\xi \tag{25}$$

Substituting Eq. (14) into Eq. (25), and the result in the left-hand side of Eq. (19), one obtains the right-hand side of Eq. (19), where

$$Cp = 1.19 \tag{26}$$

For the more general aerodynamic theory, Cp is a function of ℓ/b. For slender-body theory, $Cp \sim 1/(\ell/b)$. The general theory is discussed in Appendix B, and the function $Cp = Cp(\ell/b)$ determined. It turns out that Cp is a monotonically decreasing function of ℓ/b. Hence, using $Cp(\ell/b = 0) = 1.19$ gives a conservative estimate of the fluid velocity at which divergence occurs. The simple correction for subsonic compressibility is also discussed in Appendix B.

Numerical Results

As noted, the functional form of the solution can be expressed in terms of nondimensional parameters as follows:

$$W_0 = W_0\left(\lambda, \gamma, \ell/b, \frac{\bar{N}_x \ell^2}{D}, \frac{\bar{N}_y \ell^2}{D}\right) \tag{20}$$

Equation (20) can be expressed in more explicit terms by substituting Eqs. (17) and (19) into Eq. (16). The result can be written in compact form as a polynomial in W_0,

$$W_0^3 + C_2 W_0^2 + C_1 W_0 + C_0 = 0 \tag{27}$$

where C_0, C_1, C_2 depend on the parameters given in Eq. (20).

To illustrate the generic dependence of W_0 on these parameters, several numerical examples are considered. In each case, the results will be presented in terms of W_0 vs λ for other parameters held fixed.

Examples I_a, I_b, I_c:

$$\gamma_a, \gamma_b, \gamma_c = 0, 303.2, 3942$$

$$\ell/b = 1.857$$

$$R_x = \frac{\bar{N}_x \ell^2}{D} = 652.5$$

$$R_y = \frac{\bar{N}_y \ell^2}{D} = 351.4$$

Examples II:

$$\gamma = 3942$$

$$\ell/b = 0$$

$$R_x = \frac{\bar{N}_x \ell^2}{D} = 652.5$$

$$R_y = \frac{\bar{N}_y \ell^2}{D} = 351.4$$

Examples III:

$$\gamma = 3942$$

$$\ell/b = 1.857$$

$$\frac{\bar{N}_x \ell^2}{D} = \frac{\bar{N}_y \ell^2}{D} = 0$$

Discussion

Consider Fig. 2, which compares the results for various γ. Note the different scales used for the several γ. The generic results, most readily seen for $\gamma = 303.2$, are:

1) There is a minimum λ below which only the trivial solution $W_0 = 0$ is possible.

2) Above this λ, there are two nontrivial W_0 for some range of λ.

3) As λ increases further, one of the two possible $W_0 \to \infty$ and the other $W_0 \to 0$ as $\lambda \to \infty$.

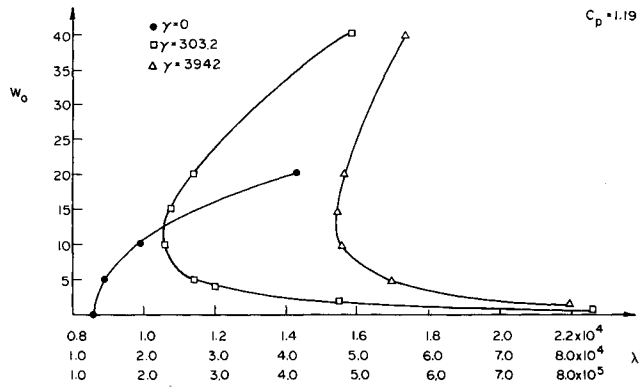

Fig. 2 Elastic shell displacement vs dynamic pressure flow parameter. Note the different horizontal scales for various curves.

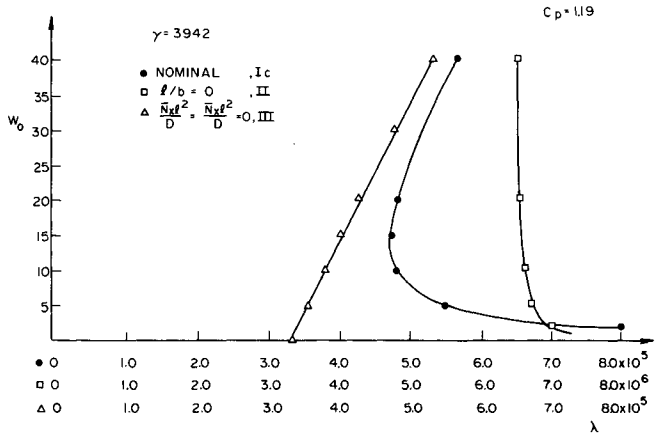

Fig. 3 Elastic shell displacement vs dynamic pressure flow parameter. Note the different horizontal scales for various curves.

4) For $\gamma = 0$, only a single nontrivial solution exists; for this case, the minimum λ for a nontrivial solution, $W_0 \neq 0$, corresponds to $W_0 \to 0$ and can be determined from a linear theory.

5) For $\gamma \neq 0$, the minimum λ for nontrivial solutions correspond to a finite W_0 and must be determined from a nonlinear theory.

Now consider γ fixed and the nominal case example I_a, along with the special cases, $\ell/b = 0$ (example II) and $\bar{N}_x = \bar{N}_y = 0$ (example III). See Fig. 3. Comparing the results from examples II and I_a, it is seen that the effect of increasing the shell width is to increase the flutter λ substantially. No qualitative change is observed, however, from the the nominal case. By contrast, if the applied in-plane loads are set to zero, $\bar{N}_x = \bar{N}_y = 0$, the minimum λ for nontrivial solutions again corresponds to $W_0 \to 0$ and can be determined from a linear theory. Moreover λ_{min} is substantially lower than for $\bar{N}_x > 0$, $\bar{N}_y > 0$. Note the different horizontal scales used in Fig. 3.

Variations in the Analytical Assumptions

In the preceding discussion, parameter variations for a given analytical model were considered. Here variations in the analytical assumptions are considered for case I_b. The previous results for this case are shown again in Fig. 4. In addition, results are shown for negative W_0 (these are not physically possible unless the mandrel is removed, but they are of mathematical interest) and the theory with the constant load term p omitted; note that the $W_0 \to 0$ result for this special case corresponds to linear theory.

These results emphasize two important points:

1) The mandrel is critical to the divergence behavior of the shell.

2) The constant load term has a stabilizing effect, which can be determined only from a nonlinear analysis. However,

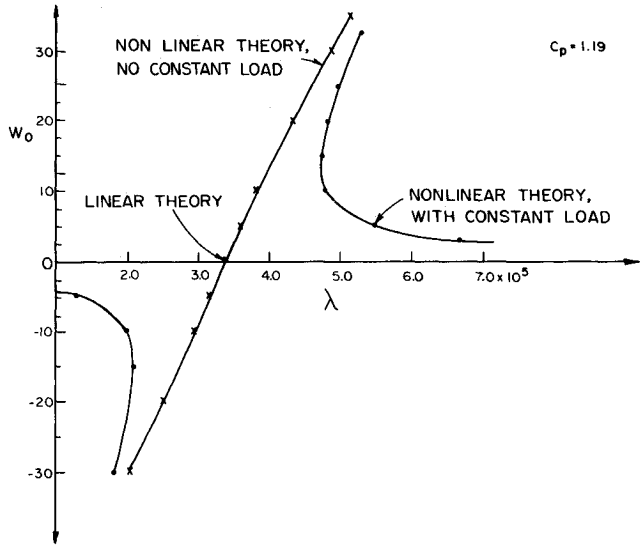

Fig. 4 Elastic shell displacement vs dynamic pressure flow parameter.

the linear theory is conservative (assuming the mandrel is in place) in that it predicts a lower velocity for divergence to occur.

Concluding Remarks

The numerical examples have illustrated the important effects of the several physical parameters and the relationship of linear to nonlinear theory. These points will not be reiterated here except to re-emphasize the essential nature of the nonlinearity and its importance to understanding the system's behavior. Two other issues will be elaborated on here.

First of all, as previously mentioned, the aerodynamic model is an approximate one, even within the framework of small-perturbation potential theory. In particular, the effect of curvature is ignored in the aerodynamic model. Moreover, the two-dimensional, incompressible aerodynamic model is used in the main text for illustrative purposes. However, the flat-plate, compressible (subsonic) three-dimensional theory is worked out in Appendix B, where it is shown that no significant qualitative differences arise due to three-dimensional or compressibility (subsonic) effects. It is anticipated that curvature will have an even smaller effect on the aerodynamic forces for the parameter range of interest.

The second issue involves determining the most critical instability mode. This is a matter of some subtlety. Throughout the text of this paper, it has been assumed that the most critical instability mode is the fundamental mode of the elastic shell. Recall Eqs. (14) and (15). Those readers familiar with the literature on the aeroelasticity of plates and shells[1] will appreciate that it is not known a priori which mode will be most critical. Indeed, it is known that within the framework of linear theory, a higher mode may be most critical for a curved plate or shell or a flat plate with large length/width ratio, ℓ/b. In Appendix C, this issue is considered in some mathematical detail within the framework of linear theory and an even more simplified form of aerodynamic "strip theory."

Here it is noted that the nonlinear stiffness provided by the mandrel will be more effective for higher modes than for the fundamental mode. Thus, heuristically, it can be argued that the fundamental mode will be most critical. More explicitly, the solution form for an arbitrary mode would replace Eqs. (14) and (15) by

$$W_{III} = w_0 \sin\frac{m\pi x}{\ell} \sin\frac{n\pi y}{b} \tag{14a}$$

$$\Phi_{III} = \Phi_0 \sin\frac{m\pi x}{\ell} \sin\frac{n\pi y}{b} \tag{15a}$$

From Eq. (14a), it is readily seen that, for $m \neq 1$ or $n \neq 1$, W_{III} will be less than zero over some portion of the mandrel surface, even when w_0 is positive. But this is not physically allowable. Hence, if the elastic shell deforms in a higher mode, it must deform in the fundamental mode, $m = n = 1$, as well, so that $W_{III} > 0$ everywhere. This suggests, though certainly does not prove, that higher modes will be less likely to be critical than the fundamental. It would be of interest to pursue this matter further, although to do so in the context of nonlinear theory would make the analysis considerably more complex.

Appendix A: In-Plane Boundary Edge Conditions and Step II

Consider Eq. (11) as an equation to determine Φ. For w, a solution will be assumed in the form

$$w = w_0 \sin\frac{\pi x}{\ell} \sin\frac{\pi y}{b} \tag{A1}$$

The solution for Φ from Eq. (11) will have both a particular part (due to w) and a homogeneous part, i.e.,

$$\Phi = \Phi_P + \Phi_H \tag{A2}$$

where, for Φ_P,

$$\Phi_P = \Phi_0 \sin\frac{\pi x}{\ell} \sin\frac{\pi y}{b} \tag{A3}$$

and, for Φ_H,

$$\Phi_H = \tfrac{1}{2}N_x^* y^2 + \tfrac{1}{2}N_y^* x^2 - N_{xy}^* xy \tag{A4}$$

Equations (A3) and (A4) are not the most general forms of the solutions but are sufficient for our purposes. Consider now two possible limiting cases for the in-plane boundary conditions, i.e., free edges and fixed edges.

Free Edges

The boundary conditions are:

$$\Phi_{yy} \equiv N_x = \bar{N}_x @ x = 0, \ell \tag{A5}$$

$$\Phi_{xx} \equiv N_y = \bar{N}_y @ y = 0, b \tag{A6}$$

$$-\Phi_{xy} \equiv N_{xy} = 0 \text{ on all edges} \tag{A7}$$

From Eqs. (A3–A6), it is deduced that

$$N_x^* = \bar{N}_x \tag{A8}$$

$$N_y^* = \bar{N}_y \tag{A9}$$

Now imposing Eq. (A7) $@ x = 0, \ell$ or $y = 0, b$ gives different conditions on N_{xy}^*. Indeed, to satisfy all of these would require a more elaborate homogeneous solution than assumed here. However, if one is content to impose a more global boundary condition than (A7), e.g.,

$$\int_0^{\ell} N_x dx \Big|_0^b = \int_0^b N_{xy} dy \Big|_0^{\ell} = 0 \tag{A8}$$

then it follows from Eqs. (A2–A4) and (A8) that $N_{xy}^* = 0$.

In sum, all of the preceding justifies setting

$$N_{x_{II}} = \bar{N}_x$$

$$N_{y_{II}} = \bar{N}_y$$

$$N_{xy_{II}} = 0$$

for free, unrestrained in-plane edges. Also, see Ref. 2.

Fixed, Immovable In-Plane Edges

From step II,

$$v_{\mathrm{II}} \neq 0$$

$$w_{\mathrm{II}_y} \neq 0$$

$$u_{\mathrm{II}} = 0$$

$$v_{\mathrm{II}_x} = 0$$

$$w_{\mathrm{II}_x} = 0 \tag{A10}$$

Thus, from Eqs. (11) and (A10), $\Phi_{P_{\mathrm{II}}} = 0$ and $N_{x_{P_{\mathrm{II}}}} = N_{y_{P_{\mathrm{II}}}} = N_{xy_{P_{\mathrm{II}}}} = 0$.

From Eq. (4) now,

$$(1-\nu^2)\frac{N_{x_{\mathrm{II}}}}{Eh} = \nu\left[v_{\mathrm{II}_y} + \frac{1}{2}(w_{\mathrm{II}_y})^2\right]$$

$$(1-\nu^2)\frac{N_{y_{\mathrm{II}}}}{Eh} = v_{\mathrm{II}_y} + \frac{1}{2}(w_{\mathrm{II}_y})^2$$

$$(1-\nu^2)\frac{N_{xy_{\mathrm{II}}}}{Eh} = 0 \tag{A11}$$

Also,

$$\Phi_{\mathrm{II}_H} = \frac{1}{2}N_x^* y^2 + \frac{1}{2}N_y^* x^2 - N_{xy}^* xy \tag{A12}$$

Recalling $N_x = \bar{N}_x$, $N_y = \bar{N}_y$, $N_{xy} = 0$, from step I for $w_{\mathrm{II}} \equiv 0$, then, from Eqs. (A11) and (A12),

$$(1-\nu^2)\frac{N_x^* - \bar{N}_x}{Eh}\,b = \nu\frac{1}{2}\int_0^b (w_{\mathrm{II}_y})^2\,dy$$

$$(1-\nu^2)\frac{N_y^* - \bar{N}_y}{Eh}\,b = \frac{1}{2}\int_0^b (w_{\mathrm{II}_y})^2\,dy \tag{A13}$$

where the following condition appropriate to fixed edges has been used to derive (A13) from (A12).

$$\int_0^b v_{\mathrm{II}_y}\,dy = 0 \tag{A14}$$

Of course, $N_{xy}^* = 0$, from Eqs. (A11) and (A12). N_x^* and N_y^* may be determined from Eq. (A13).

For real structures, the in-plane edge conditions are neither perfectly free nor fixed. However, typically, the in-plane stiffness of even thin elastic shells is large compared to that of the usual in-plane edge supports. Therefore, free edges are more nearly an accurate description than fixed edges for most practical configurations.

Appendix B: Aerodynamic Model Including Three-Dimensional Effects

For $w_y \ll 1$, the effects of spanwise curvature on the aerodynamic forces can be neglected. However, the effects of three dimensionality may be quantitatively important. Recall that the aerodynamical equations are

$$\nabla^2\phi = 0 \tag{B1}$$

$$\phi_z|_{z=0} = Uw_x \tag{B2}$$

$$\Delta p = -\rho U\phi_x \tag{B3}$$

We shall obtain a solution by using a double Fourier transform with respect to x and y.

Define the Fourier transforms of ϕ, for example, as

$$\phi^* = \frac{1}{(2\pi)^2}\int_{-\infty}^{\infty}\int \phi(x,y,z)e^{-i\alpha x}e^{-i\beta y}\,dx\,dy \tag{B4}$$

Transforming Eq. (B1), it becomes

$$\phi_{zz}^* - (\alpha^2+\beta^2)\phi^* = 0 \tag{B5}$$

The solutions to this ordinary differential equation are

$$\phi^* = Ae^{-(\alpha^2+\beta^2)^{1/2}z} + Be^{+(\alpha^2+\beta^2)^{1/2}z} \tag{B6}$$

The condition of finiteness at $z \to \infty$ requires $B \equiv 0$. A is determined by employing Eq. (B6) and satisfying (the transform of) Eq. (B2).

$$A = -\frac{U(w_x)^*}{(\alpha^2+\beta^2)^{1/2}} \tag{B7}$$

Using (the transform of) Eqs. (B3), (B6), and (B7), one finally obtains a solution for Δp (after transform inversion). The result is

$$\Delta p|_{z=0} = \frac{\rho U^2}{(2\pi)^2}\int_{-\infty}^{\infty}\int \frac{(i\alpha)}{(\alpha^2+\beta^2)^{1/2}} \left[\int_0^b\int_0^\ell w_x e^{-i\alpha x}e^{-i\alpha y}\,dx\,dy\right]e^{i\alpha x}e^{i\beta y}\,d\alpha\,d\beta \tag{B8}$$

Using Eqs. (B8) and (14) in Eq. (19), one obtains an expression for Cp. The integrals in (B8) with respect to x and y are evaluated analytically, and the final form of the expression for Cp is

$$Cp = 8\pi^2\ell^2 b\int_0^\infty\int A(\alpha,\beta)\,d\alpha\,d\beta \tag{B9}$$

where

$$A(\alpha,\beta) \equiv \frac{\alpha^2}{(\alpha^2+\beta^2)^{1/2}}\,\frac{[1+\cos(\beta b)][1+\cos(\alpha\ell)]}{[\pi^2-(\alpha\ell)^2]^2[\pi^2-(\beta b)^2]^2}$$

and it is noted that A is an even function of α and β. The quadratures in Eq. (B9) have been carried out numerically. The result is shown in Fig. B1.

Using the results of this figure and recalling Eq. (19), it is seen that

$$\lambda_{2D}C_{P_{2D}} = \lambda_{3D}C_{P_{3D}} \tag{B9}$$

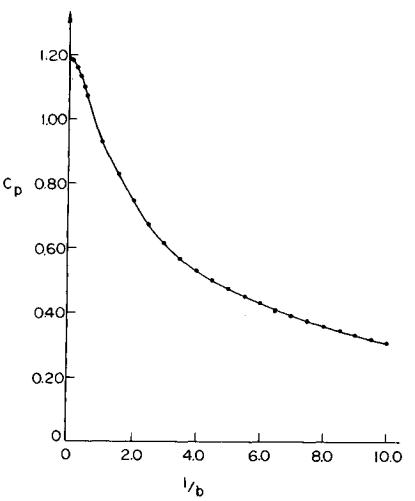

Fig. B1 Aerodynamic coefficient vs length/width.

where 2D denotes the result from the *aerodynamic model* for $\ell/b \equiv 0$ and 3D denotes the result from the aerodynamic model for $\ell/b \neq 0$. Thus, the results in the main text are by definition for λ_{2D} and $C_{P_{2D}}$. To obtain the results using the three-dimensional aerodynamic model, λ_{3D} and $C_{P_{3D}}$, we use Eq. (B9) in the form

$$\lambda_{3D} = \lambda_{2D}(C_{P_{2D}}/C_{P_{3D}})$$

where λ_{2D} is obtained from the main text analysis and $C_{P_{2D}}/C_{P_{3D}}$ is determined from Fig. B1. Thus, the three-dimensional aerodynamic effect can be thought of as simply providing a rescaling of $\lambda \sim \rho U^2$.

Finally, it is noted that the effects of compressibility can be included through a similarity law. Denoting the Mach number, $M_\infty \equiv U_\infty/a_\infty$, where a_∞ is the speed of sound in the fluid, Eq. (B1) may be generalized to

$$\beta^2\phi_{xx} + \phi_{yy} + \phi_{zz} = 0 \tag{B10}$$

where

$$\beta^2 \equiv 1 - M_\infty^2$$

and Eqs. (B2) and (B3) remain the same. By direct calculation or the method of similarity relations, it is readily shown that Eq. (B9) may be generalized to

$$\beta C_P = \beta C_P\left(\frac{\ell/b}{\beta}\right) \tag{B11}$$

Thus, Fig. B1 may also the considered to be a plot of $\beta\, C_P$ vs $[(\ell/b)/\beta]$.

The slender-body limit $[(\ell/b)/\beta] \to \infty$ can be approached by $\ell/b \to \infty$ or $\beta \to 0$. It is interesting to note that as $[(\ell/b)/\beta] \to \infty$,

$$\beta C_P \to \frac{\beta}{\ell/b}$$

or

$$C_P \to \frac{1}{\ell/b}$$

Thus, for a slender body, C_P is independent of compressibility effects, a well-known result.

The strip theory limit, $(\ell/b)/\beta \to 0$, simply states that

$$\beta C_P = 1.19$$

Note that the strip theory limit is always violated for transonic flow $\beta \to 0$, whereas all bodies of finite ℓ/b become aerodynamically "slender" as $\beta \to 0$.

Appendix C: Higher Mode, Linear Stability Analysis Using a Simplified Aerodynamic Theory

Determining the most critical mode(s) for an aeroelastic instability may pose a difficult challenge. This is true in the present case. Quite aside from the conceptual difficulty of examining all the possible modal combinations, the sheer computational labor involved may be formidable.

To illustrate the nature of the difficulties while avoiding lengthly calculations, the issue is examined here within the framework of two simplifying assumptions:

1) A classical linear stability analysis is pursued for a curved elastic plate (with the mandrel removed).

2) The aerodynamic theory is further simplified following Kornecki et al.,[3] and thus the aerodynamic pressure is taken in the form

$$\Delta p = C\rho U^2 \ell w_{xx} \tag{C1}$$

where C is a numerical constant. The critical mode will not depend on C, as will be seen, and the simplification to Eq. (C1) from Eq. (23) is not thought to have a strong effect on the critical mode either. However the strip theory assumption per se underlying Eq. (23) is not sufficiently accurate to consider all modes. As was discussed in the text, strip theory assumes that ℓ/b is sufficiently small. For arbitrary chordwise m, and spanwise n mode numbers, this can be generalized to $n\ell/mb$ sufficiently small.

The equations of equilibrium and compatibility will be simplified by neglecting all nonlinear terms. Thus in the text, Eqs. (1) and (2) become [also, see Eqs. (10_L) and (11_L) and the subsequent discussion]

$$D\nabla^4 w - \bar{N}_x w_{xx} - \bar{N}_y w_{yy} + \Phi_{xx}\left(\frac{1}{r}\right) + \Delta p = 0 \tag{C2}$$

and

$$\frac{\nabla^4\Phi}{Eh} - w_{xx}\left(\frac{1}{r}\right) = 0 \tag{C3}$$

For the solution to Eqs. (C1-C3), a more general form is assumed than before, which now allows a single, but arbitrary, chordwise and spanwise mode to be considered. Coupling between two different modes is neglected. Indeed, within the framework of Eqs. (C1-C3), it is easily shown that no coupling between modes occurs.

The assumed solution form is

$$w = w_0 \sin\frac{m\pi x}{\ell} \sin\frac{n\pi y}{b} \tag{C4}$$

$$\Phi = \Phi_0 \sin\frac{m\pi x}{\ell} \sin\frac{n\pi y}{b} \tag{C5}$$

Note that Eq. (C5) is consistent with free, unrestrained in-plane edge conditions.

Substituting Eqs. (C4) and (C5) into Eqs. (C1-C3) one generates two linear algebraic homogeneous equations for w_0 and Φ_0. The neutral stability condition is obtained by setting the determinant of coefficients of w_0 and Φ_0 to zero. Solving from this equation for the critical flow velocity for any given arbitrary mode, one obtains the following nondimensional equation:

$$\frac{C\lambda}{\pi^2} = \frac{[m^2 + n^2(\ell/b)^2]^2}{m^2} + \frac{\gamma^2}{\pi^4}\frac{m^2}{[m^2 + n^2(\ell/b)^2]^2} + \frac{R_x}{\pi^2} + \frac{R_y}{\pi^2}\frac{n^2}{m^2}\left(\frac{\ell}{b}\right)^2 \tag{C6}$$

For simplicity, consider $R_x = R_y = 0$. Then, Eq. (C6) becomes, in a convenient, compact form,

$$\tilde{\lambda} = X + \frac{\Gamma}{X} \tag{C7}$$

where

$$\tilde{\lambda} \equiv \frac{C\lambda}{\pi^2} \tag{C8a}$$

$$\Gamma \equiv \frac{\gamma^2}{\pi^4} \tag{C8b}$$

$$X \equiv \left[m^2 + n^2\left(\frac{\ell}{b}\right)^2\right]^2 \Big/ m^2 \tag{C8c}$$

From Eq. (C7), the minimum $\tilde{\lambda}$ occurs for

$$X = \Gamma^{1/2} \tag{C9}$$

and

$$\tilde{\lambda}_{\min} = 2(\Gamma)^{1/2} \tag{C10}$$

Of course, strictly speaking, X can take on discrete values only for particular m and n; see Eq. (C8c). Also, note that more than one combination of m and n can give the same X and hence the same $\tilde{\lambda}_{\min}$.

To see this, consider again Eq. (C8c). Solving for n^2,

$$n^2_{\min} = \frac{(\Gamma)^{1/4}m - m^2}{(\ell/b)^2} \tag{C11}$$

where Eq. (C9) has also been used. Here $n_{\min}$ means that this is the value of n (for a given m) that leads to $\tilde{\lambda}_{\min}$ as given by Eq. (C10).

A numerical example, such as Table 1, for $\gamma = 3942$, may help illustrate these results. Of course, $n_{\min}$ must be an integer value, and so these results are indicative only of general trends. To obtain more specific results, return to Eq. (C6), and consider Table 2. The results of Table 2 are consistent with those of Table 1.

Finally, note that, for sufficiently small γ or Γ, $m = n = 1$ gives one of the most critical modes.

All of this suggests that careful attention needs to be given to the most critical mode in a practical design application.

Table 1 Miminal n for divergence dynamic pressure

$\Gamma = 159535$	m	$n_{\min}$
$X = 399$	1	2.3
$\tilde{\lambda}_{\min} = 798$	2	3.2
	3	3.8
	etc.	

Table 2 Divergence dynamic pressure for various mode numbers

$\Gamma = 159535$	$\tilde{\lambda} = 8080$	$m = 1$	$n = 1$
	920	1	2
	1182	1	3
	3207	1	4
	11514	2	1
	2094	2	2
	827	2	3
	1059	2	4
	etc.		

Fortunately, for reasons discussed in the text, the nonlinear stiffness provided by the mandrel will raise the critical γ for the higher modes more than that for the fundamental mode, $m = n = 1$. Thus, the latter is apt to be the most critical. However, a physical experiment would be most reassuring here.

Acknowledgments

The authors would like to thank George Ku and Henry Obremski for stimulating discussions of this work. The research was supported, in part, by ARO Grant DAAL03-87-K-0023. Dr. Gary Anderson is the technical monitor.

References

[1]Dowell, E. H., *Aeroelasticity of Plates and Shells,* Kluwer, The Netherlands, 1975.

[2]Dowell, E. H. and Ventres, C. S., "Modal Equations for the Nonlinear Flexural Vibrations of a Cylindrical Shell," *International Journal of Solids, and Structures,* Vol. 4, 1968, pp. 975–991.

[3]Kornecki, A., Dowell, E. H., and O'Brien, J., "On the Aeroelastic Instability of Two-Dimensional Panels in Uniform Incompressible Flow," *Journal of Sound Vibration,* Vol. 47, No. 2, 1976, pp. 163–178.

[4]Dowell, E. H., Curtiss, H. C., Jr., Scanlan, R. H., and Sisto, F., *A Modern Course in Aeroelasticity,* 2nd ed., Kluwer, The Netherlands, 1989.